PHYSICAL REVIEW A **77**, 052711 (2008)

# Decisive role of rotational couplings in the dissociative recombination and superelastic collisions of $H_2^+$ with low-energy electrons

Ousmanou Motapon
*ICTP, Strada Costiera 11, 34014 Trieste, Italy*
*and Department of Physics, Faculty of Science, University of Douala, P.O. Box 24157, Douala, Cameroon*

Francois Olivier Waffeu Tamo
*Centre for Atomic Molecular Physics and Quantum Optics (CEPAMOQ), Faculty of Science, University of Douala, P.O. Box 8580, Douala, Cameroon*
*and Laboratoire de Mécanique, Physique et Géosciences, UFR Sciences et Techniques, Université du Havre, 25, rue Philippe Lebon, Boîte Postale 540, 76058, Le Havre, France*

Xavier Urbain
*Laboratoire PAMO, Université Catholique de Louvain, chemin du cyclotron 2, 1348, Louvain-La-Neuve, Belgium*

Ioan F. Schneider
*Laboratoire de Mécanique, Physique et Géosciences, UFR Sciences et Techniques, Université du Havre, 25, rue Philippe Lebon, Boîte Postale 540, 76058, Le Havre, France*

(Received 28 December 2007; published 20 May 2008)

The multichannel quantum-defect theory is used to investigate the role of the numerous couplings between rovibrational states in the dissociative recombination and superelastic collisions of $H_2^+$ with low-energy electrons, within different molecular electronic symmetries. All the paths accessible are considered. In the case of the singlet gerade symmetry of the neutral system, for example, not only the dominant path, $^1\Sigma_g^+$, is taken into account, but also $^1\Pi_g^+$, rotationally coupled to $^1\Sigma_g^+$, via a frame transformation from the interaction region to the external one. The initial vibrational states investigated are $v_i^+=0-4$. The final rate coefficients are obtained as weighted sums including the so-called ortho-para effect, at room temperature, over all the relevant rotational initial states $N_i^+$, which vary from 0 to 12. The results show that the consideration of rotational effects give a much better overall agreement of the dissociative recombination rate coefficients with experiment, and that, for superelastic collisions, these effects can be used to account, at least partly, for the discrepancies between our former calculations and experiment, which showed a strong vibrational relaxation of $H_2^+$.

DOI: 10.1103/PhysRevA.77.052711 PACS number(s): 34.80.Ht, 34.50.Ez, 34.80.Lx, 34.50.Gb

## I. INTRODUCTION

The dissociative recombination (DR) of $H_2^+$,

$$H_2^+ + e^- \rightarrow H + H^*, \tag{1}$$

is not only the simplest chemical reaction, but also an important process in cold astrophysical environments and laboratory and fusion edge plasmas. Sustained experimental and theoretical effort on this process resulted in the early 1990s in a reasonable agreement with merged beam measurements [1–3].

However, the advent of heavy-ion storage rings [4–8] in the electron-cation collision research area generated a revival of the interest in DR—in general—but also in the study of the benchmark process (1). Indeed, this technique allowed for better statistics, better accuracy, and, above all, vibrational resolution.

This last feature explains why most of the experimental effort has been focused on the $HD^+$ isotope [4,9–15]—rapidly relaxing during the tens of seconds of storage time—rather than on $H_2^+$. The most spectacular results on $HD^+$ concerned the low energy region, characterized by numerous resonances.

In order to understand and properly assign the resonances revealed by experiment, the theoretical approach included the *rotational* structure and corresponding interactions. Although first implemented on $H_2^+$ [16], the first validation of the rotational approach by comparison with the experimental results was performed for $HD^+$ [17], and most of the subsequent theoretical work was dedicated to this isotopomer [15,18–21].

A careful comparison between theory—rotational effects being neglected—and experiment on $H_2^+$ DR was performed some years ago [22], following prior experimental studies at the TSR storage ring in Heidelberg [23,24]. Although the order of magnitude of the theoretical DR cross section matched the experimental results, the shapes were in disagreement. More dramatically, the theoretical cross sections of superelastic collisions (SECs),

$$H_2^+(v_i^+) + e^- \rightarrow H_2^+(v_f^+ < v_i^+) + e^- \tag{2}$$

($v_i^+$ and $v_f^+$ standing for the initial and final vibrational quantum number of the ion target) were significantly lower than the experimental ones.

These facts have pushed us to reconsider the $H_2^+$-electron reactive collisions, starting from the available rotational approach already successfully employed for $\mathrm{HD}^+$. Moreover, the decisive involvement of the vibrationally excited states in SECs determined us to improve this approach, as shown below.

Up to now, as far as we know, the calculations on the dissociative recombination of ground-state $\mathrm{H}_2{}^+$ and $\mathrm{HD}^+$ with low-energy electrons have been focused on the contribution of the ${}^1\Sigma_g^+$ symmetry, which was assumed to be the dominant one, and the strength of the Rydberg-valence interaction within the ${}^1\Pi_g$ and ${}^1\Delta_g$ symmetries—coupled to ${}^1\Sigma_g^+$ via the frame transformation from the interaction region to the asymptotic one—has been systematically neglected, due to the unfavorable crossings between neutral dissociative and ion potentials. The same argument has been invoked for the neglect of the contribution of the doubly excited states pertaining to the other relevant symmetries—${}^3\Pi_g$, ${}^1\Sigma_u^+$, ${}^3\Sigma_u^+$—converging to $\mathrm{H}(1s)+\mathrm{H}(n=2)$. This is certainly justified if we restrict ourselves to the direct process only, occurring for a vibrationally ground or weakly excited cation recombining with a low-energy electron, but breaks down beyond this context. Indeed, when the indirect process is possible, it takes place via rovibrationally excited Rydberg states, and the higher the vibrational excitation, the better the overlap between the ionic core wave functions and the wave functions of the excited valence states, compensating the small electronic interactions and making the role of the low vibrational levels much less relevant.

The above considerations are still more pertinent in the case of the DR of vibrationally excited ions, and of the inelastic and superelastic collisions. In this latter case, the Rydberg-valence interactions are further amplified by the double occurrence of the highly excited vibrational states—the initial excitation of the target being coupled to the final one, via the dissociative resonant state. Therefore, rotational effects are likely to be more important for these processes than for DR.

## II. SUMMARY OF THE METHOD

The present work accounts for all the relevant symmetries. It is based on the extension of the original multichannel quantum-defect theory (MQDT) treatment of DR [25] toward the account of rotational structure and interactions [15,16,18,26,27,32,36]. This approach has been applied to $\mathrm{HD}^+$, $\mathrm{H}_2{}^+$, and $\mathrm{NO}^+$, so far restricted to the account of one single electronic symmetry [15–21]. In the cases of interest for this study, the DR, together with the competitive elastic, inelastic, and superelastic collisions, occurs mainly through the electronic interaction between the ground-state ion $(1s\sigma_g\, X\, {}^2\Sigma_g^+)$+incoming electron initial configurations, on one hand, and the lowest doubly excited states, on the other hand. These latter states belong to the $Q_1$ Rydberg series converging to the first excited electronic state of the ion $(2p\sigma_u\, {}^2\Sigma_u^+)$ [29,30].

The MQDT approach is based on a description of molecular states in which only part of the electronic Hamiltonian is diagonalized, within subspaces of electronic states of similar nature. We use a quasidiabatic representation of molecular states [28] to cope with problems due to the avoided crossings of the potential energy curves. The short-range electronic interactions between states of different subspaces are then found out in terms of an electronic coupling operator $\mathcal{V}$ which couples the ionization channels (Rydberg states and electron-ion states from the ionization continuum) to the dissociative channels (valence states). Starting from $\mathcal{V}$, one builds the short-range reaction matrix $\mathcal{K}$, solution of the Lippmann-Schwinger integro-differential equation:

$$\mathcal{K} = \mathcal{V} + \mathcal{V}\frac{\mathbf{1}}{\boldsymbol{E} - \boldsymbol{H}_0}\mathcal{K}, \qquad (3)$$

$\boldsymbol{H}_0$ being the zero-order Hamiltonian associated with the molecular system, i.e., the Hamiltonian operator excluding the interaction potential $\mathcal{V}$. The effects of short-range interaction are valid in the region of small electron-ion and nucleus-nucleus distances, that is, the "*A* region" [26] where the Born-Oppenheimer representation is appropriate for the description of the colliding system. There, the energy dependence of the electronic couplings can be neglected. In the case of weak coupling, a perturbative solution of Eq. (3) can be obtained. This solution has been recently proven to be exact to second order, in the case of energy-independent electronic coupling [31].

In the external zone, the "*B* region" [26] represented by large electron-core distances, the Born-Oppenheimer model is no longer valid for the ionization channels and a close-coupling representation in terms of the molecular ion+electron is more appropriate.

A complete analysis, accounting for the direct and indirect mechanisms, and for the rovibrational structure and interactions, can be summarized as follows: starting from a given rovibrational level $(N_i^+,\ v_i^+)$ of the ion initial electronic state, several values $N$ of the total angular momentum of the neutral molecule can be formed by coupling the ionic angular momentum with a specific partial wave $l$ of the incoming electron. Each $N$ value is a good quantum number conserved during the whole process and is involved in a separate calculation, leading to partial DR cross sections which are then summed up to yield the total cross section. Within each $N$ subspace, rotation is included through a frame transformation [18,27,32] between coupling schemes corresponding to the incident electron being decoupled from (external region) or coupled to (internal region) the core electrons. This frame transformation mixes the different quantum numbers compatible with a given set of $(N_i^+,\ l,\ N)$ values. The channel mixing coefficients involve angular coupling coefficients combined with electronic and vibrational factors:

$$\begin{aligned}\mathcal{C}_{lN^+v^+,\Lambda\alpha} &= \left(\frac{2N^+ + 1}{2N + 1}\right)^{1/2}\langle l(\Lambda - \Lambda^+)N^+\Lambda^+|lN^+N\Lambda\rangle\\ &\quad\times\frac{1 + \tau^+\tau(-1)^{N-l-N^+}}{[2(2 - \delta_{\Lambda^+,0})(1 + \delta_{\Lambda^+,0}\delta_{\Lambda,0})]^{1/2}}\\ &\quad\times\sum_v U_{lv,\alpha}^{\Lambda}\langle\chi_{N^+v^+}^{\Lambda^+}|\cos[\pi\mu_l^{\Lambda}(R) + \eta_\alpha^{\Lambda}]|\chi_{Nv}^{\Lambda}\rangle, \qquad (4)\end{aligned}$$

$$\mathcal{C}_{d_j,\Lambda\alpha} = U^{\Lambda}_{d_j\alpha}\cos\eta^{\Lambda}_{\alpha}, \tag{5}$$

as well as $\mathcal{S}_{lN^+v^+,\Lambda\alpha}$ and $\mathcal{S}_{d_j,\Lambda\alpha}$, obtained by replacing cosine by sine in Eqs. (4) and (5). In the preceding formulas, $\chi^{\Lambda^+}_{N^+v^+}$ is a vibrational wave function of the molecular ion, and $\chi^{\Lambda}_{Nv}$ is a vibrational wave function of the neutral system adapted to the interaction ($A$) region. The quantities $\tau^+$ and $\tau$ are related to the reflection symmetry of the ion and neutral wave functions, respectively, and take the values +1 for symmetric states and −1 for antisymmetric ones. The ratio in front of the sum in the right-hand side of Eq. (4) contains the selection rules for the rotational quantum numbers. The indices $d_j$ ($j=0,1,2,\ldots$) stand for the states of a given symmetry, open to dissociation at the current energy. $\alpha$ denotes the eigenchannels built through the diagonalization of the reaction matrix $\mathcal{K}$, and $-\tan(\eta^{\Lambda}_{\alpha})/\pi$ and $U^{\Lambda}_{lv,\alpha}$ are its eigenvalues and the components of its eigenvectors, respectively.

The projection coefficients shown in (4) and (5) include the two types of couplings controlling the process: the electronic coupling, expressed by the elements of the matrices $\boldsymbol{U}$ and $\boldsymbol{\eta}$, and the nonadiabatic coupling between the ionization channels, expressed by the matrix elements involving the quantum defect $\mu^{\Lambda}_{l}$. This latter interaction is favored by the variation of the quantum defect with the internuclear distance $R$. The matrices $\mathcal{C}$ and $\mathcal{S}$ with elements (4) and (5) are the building blocks of the "generalized" scattering matrix $\boldsymbol{X}$:

$$\boldsymbol{X} = \frac{\mathcal{C} + i\mathcal{S}}{\mathcal{C} - i\mathcal{S}}. \tag{6}$$

Since no rotational coupling between different $\Lambda$ symmetries is available in the reaction region, the reaction matrix $\mathcal{K}$ is block diagonal, relying on blocks $\mathcal{K}^{\Lambda}$, associated with $\Lambda=0,1$, etc. For a given symmetry of the neutral—defined by the spin quantum number and by the behavior with respect to reflection (+ or −) and nuclei inversion ($g$ or $u$)—the generalized scattering matrix $\boldsymbol{X}$ is built from contributions pertaining to all the $\Lambda$ subspaces, whereas the physical scattering matrix, restricted to the *open* channels, is given by [33]

$$\boldsymbol{S} = \boldsymbol{X}_{oo} - \boldsymbol{X}_{oc}\frac{1}{\boldsymbol{X}_{cc} - \exp(-i2\pi\boldsymbol{\nu})}\boldsymbol{X}_{co}. \tag{7}$$

It is obtained from the submatrices of $\boldsymbol{X}$ involving the lines and columns associated with the open (o) and closed (c) channels, and a further diagonal matrix $\boldsymbol{\nu}$ formed with the effective quantum numbers $\nu_{N^+v^+}=[2(E_{N^+v^+}-E)]^{-1/2}$ (in atomic units) associated with each vibrational threshold $E_{N^+v^+}$ of the ion situated above the current energy $E$ (and consequently labeling a *closed* channel).

For a molecular ion initially on the level $N_i^+v_i^+$ and recombining with an electron of energy $\varepsilon$, the cross section of capture into all the dissociative states $d_j$ of the same symmetry is given by

$$\sigma^{N,sym}_{diss\leftarrow N_i^+v_i^+} = \frac{\pi}{4\varepsilon}\frac{2N+1}{2N_i^+ + 1}\rho^{sym}\sum_{l,\Lambda,j}|S^{N\Lambda}_{d_j,lN_i^+v_i^+}|^2 \tag{8}$$

and the cross section for a rovibrational transition to the final level $N_f^+v_f^+$ is

$$\sigma^{N,sym}_{N_f^+v_f^+\leftarrow N_i^+v_i^+} = \frac{\pi}{4\varepsilon}\frac{2N+1}{2N_i^+ + 1}\rho^{sym}\sum_{l,l',\Lambda,j}|S^{N\Lambda}_{N_f^+v_f^+l',N_i^+v_i^+l}|^2. \tag{9}$$

Here $\rho^{sym}$ is the ratio between the multiplicities of the neutral and the target ion. After performing the MQDT calculation for all the accessible total rotational quantum numbers $N$ and for all the relevant symmetries, one has to sum up the corresponding cross sections in order to obtain the global cross section for dissociative recombination or rovibrational transition.

## III. COMPUTATIONS

Since the lower $^1\Delta_g$ electronic potential curve correlates with the H(1$s$)+H(3$l$) limit, too high with respect to the energy range currently explored, we restricted ourselves to the contribution of the states of $\Sigma$ and $\Pi$ symmetry. As a consequence of the consideration of rotational effects, the $^1\Pi_g$ state will split into two states [26]: on one hand the $^1\Pi_g^+$, symmetric with respect to reflection, simultaneously involved with $^1\Sigma_g^+$ in the frame transformation in the outer region, and on the other hand, the $^1\Pi_g^-$, antisymmetric. The same considerations hold for all the $^{1,3}\Sigma,\Pi_{g,u}$ states. Since the ions are not rotationally resolved, the actual vibrational transition cross section is obtained as a weighted sum at room temperature (300 K) over the initial rotational numbers of the vibrational level of interest. In the case of $H_2{}^+$, the consideration of the ortho-para effect, due to the distinction of the symmetric and antisymmetric nuclear spin states, leads to a weighted sum [34,35] over the odd and even values of $N_i^+$, the parity of which is associated with a specific statistical weight which is common to either $g^+$ and $u^-$ symmetries, or $g^-$ and $u^+$ symmetries. A Boltzmann distribution is assumed for the probabilities of the various rotational states, and the excitation energy is taken with respect to the lowest rotational level of the corresponding initial vibrational level, in the even and odd cases, i.e., $(E_{v_i^+N_i^+}-E_{v_i^+,0})$ or $(E_{v_i^+N_i^+}-E_{v_i^+,1})$. Actually, for a Boltzmann distribution and for the temperature of interest, rotational levels higher than $N_i^+=12$ are negligible.

We have studied the DR and SEC reactions through the lowest molecular doubly excited electronic states of the $Q_1$ group, of symmetry $^1\Sigma_g^+$, $^3\Sigma_g^+$, $^1\Pi_g$, $^3\Pi_g$, $^1\Sigma_u^+$, and $^3\Sigma_u^+$, converging to H(1$s$)+H($n$=2). The incident electron's partial waves efficiently coupled to the dissociation channels are $l=0$ or $l=2$ for a fragmentation via a $^1\Sigma_g^+$ state, $l=2$ via a $^1\Pi_g$ or $^3\Pi_g$ state, and $l=1$ via a $^1\Sigma_u^+$ or $^3\Sigma_u^+$, whereas the $^3\Sigma_g^+$ symmetry displays negligible Rydberg-valence coupling, and, consequently, its contribution was neglected [30].

For the $^1\Sigma_g^+$ symmetry, we have improved the quasidiabatic molecular data—dissociative potential curve, electronic couplings, and quantum defects—previously used [22], in order to fit a larger set of adiabatic potential energy curves [37]. This least-square adjustment, similar to that employed by Ross and Jungen [38], was performed by building up a set of diabatic Rydberg potentials in the $s$ and $d$ series, which after diagonalization of the Hamiltonian matrix containing scaled electronic couplings, reproduced the adiabatic

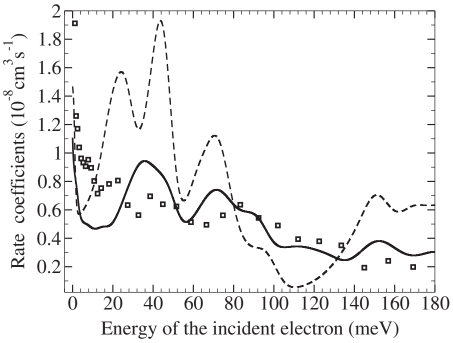

FIG. 1. Rate coefficients for dissociative recombination from $v_i^+=0$. Dashed line, theory without rotation [22]; full line, theory with rotation; squares, experiment [24]. Better agreement with experiment is found in the rotational case. Also a sensitivity with respect to the quantum defect is observed.

energies with minimal deviation. The dissociative curve obtained in the same process was further constrained at short internuclear distance by including the electronic scattering calculations of Tennyson [30] in the set of adiabatic potential curves, while the electronic couplings were kept in agreement with the total autoionization width provided by the scattering calcualtions.

As for the other symmetries, we have used the same electronic energies and couplings as before [22], but more recently computed quantum defects [30]. The $\mathcal{K}$ matrix is built up, for each symmetry, by resolution of the Lippmann-Schwinger equation to second order of the perturbation theory, which was found to provide exact solutions in the case of energy-independent electronic coupling [31].

## IV. RESULTS AND DISCUSSION

We plot in Fig. 1 the rate coefficients for dissociative recombination from $v_i^+=0$, compared to the nonrotational calculations and experiment. One may notice that the account of the rotational effects considerably increases the agreement with the measurements—in magnitude and shape—with respect to the previous nonrotational modeling. The inclusion of rotational structure and interactions results in a remarkable change in the modeling of the dynamics, dominated by resonant temporary captures into Rydberg states. For a given symmetry—e.g., ${}^1\Sigma_g^+$—the Rydberg-valence coupling is distributed in a different way within the numerous states, in comparison with the nonrotational case. Moreover, the *incoherent* sum of contributions coming from different symmetries—e.g., ${}^1\Sigma_g^+$ and ${}^1\Pi_g^+$—in the nonrotational case is replaced, in the rotational one, by a *coherent* sum, due to the channel mixing through the frame transformation—formulas (4) and (5). This results in mutual assistance between the symmetries, which means, for example, that part of the contribution to the cross section of the ${}^1\Sigma_g^+$ channels is used to feed the ${}^1\Pi_g^+$ ones, and vice versa. This explains why, in the leftmost region of Fig. 1, the result without rotation displays two peaks, while that accounting for rotation displays one peak only.

Figure 2 presents the rate coefficients for DR and SECs from the initial vibrational level $v_i^+=1$. Surprisingly, for DR, the nonrotational calculations seem to result in better agreement with experiment, in comparison with the rotational ones. However, the comparison is available for one single energy only, and the present rotational results at this point still agree with the measurements within the very large experimental error bar. One may notice that the ${}^1\Sigma_g^+$ and ${}^1\Pi_g^+$ symmetries strongly dominate the process, the role of the other symmetries (${}^1\Pi_g^-, {}^3\Pi_g, {}^1\Sigma_u^+, {}^3\Sigma_u^+$) being negligible. In the left side of Fig. 2, the absence of the dip in the rotational case is due to the same mutual enhancement between rotationally coupled symmetries as that described in the preceding paragraph.

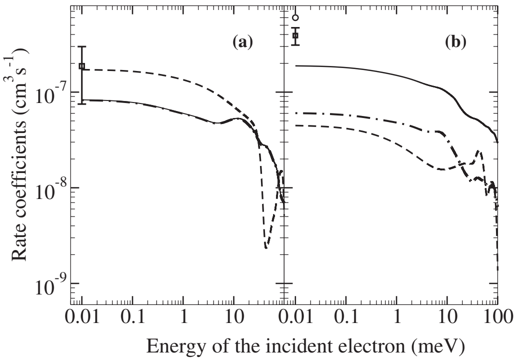

FIG. 2. Rate coefficients for (a) dissociative recombination and (b) superelastic collisions from $v_i^+=1$. Dashed lines, theory without rotation [22]; dash-dotted lines, theory with rotation for ${}^1\Sigma_g^+ + {}^1\Pi_g$; full black lines, theory with rotation for all symmetries; squares, experiment [24]; circle, experiment [23].

As for SECs, the rotational effects strongly increase the rate coefficient. More specifically, the account in the rotational context of the two frame-transformation-coupled symmetries ${}^1\Sigma_g^+$ and ${}^1\Pi_g^+$ introduces a factor of about 1.5 between the old and the new rate coefficients at "zero" energy. Moreover, the account of the other relevant symmetries—${}^1\Pi_g$, ${}^3\Pi_g$, ${}^1\Sigma_u^+$, ${}^3\Sigma_u^+$—results in a global factor of about 5.

The explanation for this strong rotational effect resides—as shown in numerous recent studies [39–44]—in the channel mixing, mostly driven in this case by the indirect process. Indeed, whereas the lowest (${}^1\Sigma_g^+$) doubly excited state crosses the ion curve close to $v^+=1$, all the other doubly excited states (pertaining to the other symmetries) experience this crossing close to much higher vibrational levels, accessible either by vibronic coupling between the ionization channels or by successive Rydberg-valence couplings [45].

TABLE I. Rate coefficients for dissociative recombination of $H_2^+$ with electrons of near-zero kinetic energy.

| $v_i^+$ | Theory [22] ($10^{-8}$ cm$^3$/s) | Theory (this work) ($10^{-8}$ cm$^3$/s) | Experiment [24] ($10^{-8}$ cm$^3$/s) |
|---|---|---|---|
| 0 | 1.47 | 1.12 | $1.87 \pm 0.15$ |
| 1 | 17.16 | 8.31 | $18.7 \pm 11.2$ |
| 2 | 5.16 | 5.37 | $15.3 \pm 9.5$ |
| 3 | 9.61 | 16.46 | $18.0 \pm 11.5$ |
| 4 | 9.17 | 14.90 | $9.9 \pm 6.3$ |

TABLE II. Rate coefficients for superelastic collisions of $H_2^+$ with electrons of near-zero kinetic energy.

| $v \rightarrow v'$ | Experiment [23] ($10^{-8}$ cm$^3$/s) | Theory [22] ($10^{-8}$ cm$^3$/s) | Theory (this work) ($10^{-8}$ cm$^3$/s) | Experiment [24] ($10^{-8}$ cm$^3$/s) |
|---|---|---|---|---|
| $1 \rightarrow 0$ | 60 | 4.47 | 18.82 | $39 \pm 8$ |
| $2 \rightarrow 1$ | 120 | 16.95 | 38.48 | $76 \pm 16$ |
| $2 \rightarrow 0$ | | 3.15 | 3.48 | |
| $3 \rightarrow 2$ | 220 | 9.61 | 52.16 | $121 \pm 26$ |
| $3 \rightarrow 1$ | | 6.73 | 11.42 | |
| $3 \rightarrow 0$ | | 1.70 | 1.67 | |
| $4 \rightarrow 3$ | 240 | 27.20 | 94.03 | $146 \pm 30$ |
| $4 \rightarrow 2$ | | 2.61 | 16.31 | |
| $4 \rightarrow 1$ | | 3.78 | 5.26 | |
| $4 \rightarrow 0$ | | 1.07 | 1.18 | |

When going from the purely vibrational picture to the rovibrational one, this channel mixing is considerably enhanced by the large multiplication of ionization channels and, consequently, by the corresponding large multiplication of mutual couplings between them. As a result, the involvement of ionization channels associated to highly excited vibrational levels, strongly coupled with the valence state, will "contaminate" the interaction between the entrance ionization channel and the exit one, i.e., the dissociation channel for the DR and the ionization channel for the SEC.

This effect is weak for the DR of $v^+=1$ ions, since the direct interaction between the entrance ionization channel and the exit dissociative one is the strongest possible. In contrast, the SECs of the $v^+=1$ ions proceed by a two-step interaction [25,46], relying on the $v^+=1 \rightarrow$dissociation *and* the dissociation$\rightarrow v^+=0$ couplings: it is this latter weak interaction that is strongly enhanced by the above described contamination, and this enhancement is very much favored by the abundant rovibrational channels occurring in the rotational context.

Tables I and II display the status of the present agreement between theory and experiment for "zero" energy (actually, 10 $\mu$eV detuning energy). These results are also compared with the previously computed data (corrected, as described above).

For the DR, the present and previous theoretical results roughly agree with the experiment [24] within the large error bars. For the SECs, the rotationally computed rate coefficients agree much better with those coming from the second series of experimental data [24], being considerably higher than our previous theoretical rates that did not include rotational coupling. Theory is now able to confirm the high rates of vibrational relaxation due to superelastic collisions, put in evidence by the storage-ring measurements. One may also notice that our present calculations confirm the nonnegligible role of the vibrational transitions occurring beyond the "propensity rule" $|\Delta v|=1$.

## V. CONCLUSIONS AND PERSPECTIVES

In conclusion, we show that rotational effects play a decisive role in the rapid vibrational relaxation of $H_2^+$. In comparison to the nonrotational calculations, a much better agreement of the rate coefficients has been observed with experiment for both SECs, at "zero" energy, and DR, in a broad energy range.

Very recently, new experimental results on the DR of rovibrationally resolved $H_2^+$ ions became available, in a broad range of energy [47,48]. Extensive calculations, based on the theoretical refinements described in this work, are presently in progress, in order to provide state-to-state cross sections comparable with these new measured data.

## ACKNOWLEDGMENTS

The authors thank Professor A. Suzor-Weiner, Professor Christian Jungen, Professor Chris Green, and Professor Andreas Wolf for many useful discussions and scientific support. O.M. is grateful to the Abdus Salam International Centre for Theoretical Physics, where most of this work was undertaken, as well as to the Swedish International Development Agency (SIDA) for financial support. F.O.W.T. and O.M. acknowledge financial support from the French "Ministère des Affaires Etrangères (through the "Service de la Coopération et de l'Action Culturelle" of Yaoundé, Cameroon) and from the University of Le Havre. The authors acknowledge financial support from the French "Contrat de Plan Etat-Région: Combustion dans les Moteurs," Centre de Recherche Informatique de la Haute Normandie (CRIHAN), and Centre National de la Recherche Scientifique (CNRS) through GdR "Cataplasme" and "ARCHES." X.U. acknowledges financial support from the Belgian F.R.S.-FNRS. I.F.S. is grateful to the Université Catholique de Louvain and to the Japanese Society for the Promotion of Science for financial support. He is also grateful to the Max Planck Society for making possible a research visit at the Ion Storage and Molecular Quantum Dynamics laboratory of the Max-Plank-Institut für Kernphysik in Heidelberg.

[1] J. B. and A. Mitchell, Phys. Rep. **186**, 215 (1990).

[2] I. F. Schneider, O. Dulieu, and A. Giusti-Suzor, J. Phys. B **24**, L289 (1991).

[3] I. F. Schneider, O. Dulieu, and A. Giusti-Suzor, Phys. Rev. Lett. **68**, 2251 (1992).

[4] P. Forck, M. Grieser, D. Habs, A. Lampert, R. Repnow, D. Schwalm, A. Wolf, and D. Zajfman, Phys. Rev. Lett. **70**, 426 (1993).

[5] M. Larsson, H. Danared, J. R. Mowat, P. Sigray, G. Sundström, L. Broström, A. Filevich, A. Källberg, S. Mannervik, K. G. Rensfelt, and S. Datz, Phys. Rev. Lett. **70**, 430 (1993).

[6] T. Tanabe, I. Katayama, N. Inoue, K. Chida, Y. Arakaki, T. Watanabe, M. Yoshizawa, S. Ohtani, and K. Noda, Phys. Rev. Lett. **70**, 422 (1993).

[7] J. Richard Mowat, H. Danared, G. Sundstrom, M. Carlson, L. H. Andersen, L. Vejby-Christensen, M. af Ugglas, and M. Larsson, Phys. Rev. Lett. **74**, 50 (1995).

[8] D. Zajfman, A. Wolf, D. Schwalm, D. A. Orlov, M. Grieser, R. von Hahn, C. P. Welsch, J. R. Crespo Lopez-Urrutia, C. D. Schröter, X. Urbain, and J. Ullrich, J. Phys.: Conf. Ser. **4**, 296 (2005).

[9] C. Strömholm, I. F. Schneider, G. Sundström, L. Carata, H. Danared, S. Datz, O. Dulieu, A. Källberg, M. af Ugglas, X. Urbain, V. Zengin, A. Suzor-Weiner, and M. Larsson, Phys. Rev. A **52**, R4320 (1995).

[10] T. Tanabe *et al.*, J. Phys. B **32**, 5221 (1999).

[11] L. H. Andersen, P. J. Johnson, D. Kella, H. B. Pedersen, and L. Vejby-Christensen, Phys. Rev. A **55**, 2799 (1997).

[12] A. Al-Khalili *et al.*, J. Chem. Phys. **121**, 5700 (2004).

[13] Z. Amitay, A. Baer, M. Dahan, L. Knoll, M. Lange, J. Levin, I. F. Schneider, D. Schwalm, A. Suzor-Weiner, Z. Vager, R. Wester, and D. Zajfman, Science **281**, 75 (1998).

[14] Z. Amitay, A. Baer, M. Dahan, J. Levin, Z. Vager, D. Zajfman, L. Knoll, M. Lange, D. Schwalm, R. Wester, A. Wolf, I. F. Schneider, and A. Suzor-Weiner, Phys. Rev. A **60**, 3769 (1999).

[15] I. F. Schneider, C. Strömholm, L. Carata, X. Urbain, M. Larsson, and A. Suzor-Weiner, J. Phys. B **30**, 2687 (1997).

[16] H. Takagi, J. Phys. B **26**, 4815 (1993).

[17] T. Tanabe, I. Katayama, H. Kamegaya, K. Chida, Y. Arakaki, T. Watanabe, M. Yoshizawa, M. Saito, Y. Haruyama, K. Hosono, K. Hatanaka, T. Honma, K. Noda, S. Ohtani, and H. Takagi, Phys. Rev. Lett. **75**, 1066 (1995).

[18] B. Vâlcu, I. F. Schneider, M. Raoult, C. Strömholm, M. Larsson, and A. Suzor-Weiner, Eur. Phys. J. D **1**, 71 (1998).

[19] H. Takagi, in *Dissociative Recombination: Theory, Experiment and Applications IV*, edited by M. Larsson, J. B. A. Mitchell, and I. F. Schneider (World Scientific, Singapore, 2000), p. 180.

[20] H. Takagi, Phys. Scr. T **96**, 52 (2002).

[21] M. C. Stroe, A. I. Florescu, M. Fifirig, F. O. Waffeu Tamo, V. Ngassam, O. Motapon, and I. F. Schneider, Rom. Rep. Phys. **57**, 801 (2005).

[22] V. Ngassam, O. Motapon, A. Florescu, L. Pichl, I. F. Schneider, and A. Suzor-Weiner, Phys. Rev. A **68**, 032704 (2003).

[23] S. Krohn, Z. Amitay, A. Baer, D. Zajfman, M. Lange, L. Knoll, J. Levin, D. Schwalm, R. Wester, and A. Wolf, Phys. Rev. A **62**, 032713 (2000).

[24] S. Krohn, Ph.D. thesis, University of Heidelberg, 2001, http://www.ub.uni-heidelberg.de/archiv/1826

[25] A. Giusti, J. Phys. B **13**, 3867 (1980).

[26] C. Jungen and O. Atabek, J. Chem. Phys. **66**, 5584 (1977).

[27] U. Fano, Phys. Rev. A **2**, 353 (1970).

[28] V. Sidis and H. Lefèbvre-Brion, J. Phys. B **4**, 1040 (1971).

[29] S. L. Guberman, J. Chem. Phys. **78**, 1404 (1983).

[30] J. Tennyson, At. Data Nucl. Data Tables **64**, 253 (1996).

[31] V. Ngassam, A. Florescu, L. Pichl, I. F. Schneider, O. Motapon, and A. Suzor-Weiner, Eur. Phys. J. D **26**, 165 (2003).

[32] E. S. Chang and U. Fano, Phys. Rev. A **6**, 173 (1972).

[33] M. J. Seaton, Rep. Prog. Phys. **46**, 167 (1983).

[34] B. H. Bransden and C. J. Joachain, *Physics of Atoms and Molecules*, 2nd ed. (Prentice-Hall, London, 2003), pp. 562–563.

[35] I. F. Schneider, O. Dulieu, A. Giusti-Suzor, and E. Roueff, Astrophys. J. **424**, 983 (1994).

[36] H. Takagi, N. Kosugi, and M. Le Dourneuf, J. Phys. B **24**, 711 (1991).

[37] T. Detmer, P. Schmelcher, and L. Cederbaum, Phys. Rev. A **57**, 1767 (1998).

[38] S. Ross and Ch. Jungen, Phys. Rev. Lett. **59**, 1297 (1987).

[39] I. F. Schneider, A. E. Orel, and A. Suzor-Weiner, Phys. Rev. Lett. **85**, 3785 (2000).

[40] I. F. Schneider, I. Rabadán, L. Carata, L. H. Andersen, A. Suzor-Weiner, and J. Tennyson, J. Phys. B **33**, 4849 (2000).

[41] I. F. Schneider and A. Suzor-Weiner, Phys. Essays **13**, 280 (2001).

[42] V. Kokoouline, C. H. Greene, and B. D. Esry, Nature (London) **412**, 891 (2001).

[43] S. Fonseca dos Santos, V. Kokoouline, and C. H. Greene, J. Chem. Phys. **127**, 124309 (2007).

[44] R. Curik and Ch. H. Greene, Phys. Rev. Lett. **98**, 173201 (2007).

[45] I. F. Schneider, O. Dulieu, and A. Giusti-Suzor, J. Phys. B **24**, L289 (1991).

[46] K. Nakashima, H. Takagi, and H. Nakamura, J. Chem. Phys. **86**, 726 (1987).

[47] V. Zhaunerchyk, A. Al-Khalili, R. D. Thomas, W. D. Geppert, V. Bednarska, A. Petrignani, A. Ehlerding, M. Hamberg, M. Larsson, S. Rosén, and W. J. van der Zande, Phys. Rev. Lett. **99**, 013201 (2007).

[48] N. de Ruette, Ph.D. thesis, Université Catholique de Louvain, 2007.